Copper(II) and Copper(I) Complexes Stabilized by Phosphine Oxides: Synthesis and Characterization of the Cationic Complexes $[Cu(odppf)_2(EtOH)]^{2+}$ and $[Cu(odppf)_2]^{2+}$, Precursors of the Novel Copper(I) Adduct $[Cu(odppf)_2]^{+}$ (odppf = 1,1′-Bis(oxodiphenylphosphoranyl)ferrocene). Crystal Structure of $[Cu(odppf)_2(EtOH)](BF_4)_2$ and $[Cu(odppf)_2](BF_4)_2$

Giuseppe Pilloni,*,† Giovanni Valle,‡ Carlo Corvaja,§ Bruno Longato,†,|| and Benedetto Corain||,⊥

Dipartimento di Chimica Inorganica, Metallorganica e Analitica, Università di Padova, Via Marzolo 1, 35131 Padova, Italy, Centro di Ricerca sui Biopolimeri, CNR, Dipartimento di Chimica Organica, Università di Padova, Via Marzolo 1, 35131 Padova, Italy, Dipartimento di Chimica Fisica, Università di Padova, Via Loredan 2, 35131 Padova, Italy, Centro di Ricerca sulla Stabilità e Reattività dei Composti di Coordinazione, CNR, Via Marzolo 1, 35131 Padova, Italy, and Dipartimento di Chimica, Ingegneria Chimica e Materiali, Università de L'Aquila, Via Vetoio, 67010 L'Aquila, Italy

Received February 9, 1995[⊗]

The ferrocenylbis(phosphine) dioxide complexes $[Cu(odppf)_2(EtOH)](BF_4)_2$ (**1**) and $[Cu(odppf)_2](BF_4)_2$ (**2**) (odppf = 1,1′-bis(oxodiphenylphosphoranyl)ferrocene) have been prepared and characterized in the solid state by X-ray analysis and in solution by a combination of ESR, visible, and IR spectroscopies and electrochemical techniques. The complexes crystallize in the monoclinic system, space group $P2_1/c$, with $Z = 4$, and $a = 19.484(2)$ and 12.325(2) Å, $b = 13.450(2)$ and 33.137(3) Å, $c = 25.477(2)$ and 17.608(2) Å, and $\beta = 93.9(1)$ and 108.7(2)°, for complexes **1** and **2**, respectively. In the cations the four O atoms of two odppf ligands are directly bonded to the metal center with Cu−O distances ranging from 1.92 to 2.076 Å. In complex **1** the metal is pentacoordinate with the five donor atoms at the vertices of a distorted trigonal bipyramid formed by two chelated odppf moyeties and one molecule of ethanol, occupying an equatorial position, as the fifth ligand. In complex **2** the coordination geometry around the metal atom is distorted square-planar with the two odppf moieties acting as chelating ligands with a bite angle of about 153°. The lability of EtOH ligand allows complex **1** to be easily and reversibly converted into complex **2** upon dissolution in noncoordinating solvents. ESR data in frozen solution of **1** in ethanol and of **2** in dichloroethane point to the confirmation of the square-planar stereochemistry for complex **2** and to the conversion of the trigonal-bipyramidal structure of **1** into a square-pyramidal one. ESR parameters clearly indicate that *ca.* 95% of the unpaired electron resides in the metal center, thus revealing a scarcely covalent character of the Cu^{II}−O bonds. A single well-defined oxidation process involving the two ferrocene cores has been detected by cyclic voltammetry for complex **2** in dichloroethane, while two discrete single electron reductions centered on the copper atom were observed under the same conditions. The one-electron reduction product was identified as the remarkable species $[Cu(odppf)_2]^{+}$ (**3**) which, although extremely reactive toward dioxygen, turned out to be quite stable toward valence disproportionation in aprotic solvents.

Introduction

We have recently reported on the X-ray molecular structure of the ligand odppf (odppf = 1,1′-bis(oxodiphenylphosphoranyl)ferrocene) and of the copper(I) complex [Cu(dppf)(odppf)]-BF_4 (dppf = 1,1′-bis(diphenylphosphino)ferrocene) and we have shown that the ligand set $\{P_2O_2\}$ appears to be particularly well suited for stabilizing Cu^{I} toward valence disproportionation in aprotic solvents.[1]

In the frame of our ongoing interest in the coordination chemistry of dppf and odppf[1,2] we report on the synthesis, X-ray single-crystal structure, and solution-state ESR characterization as well as on the electrochemical behavior of $[Cu(odppf)_2(EtOH)](BF_4)_2$, **1**, and $[Cu(odppf)_2](BF_4)_2$, **2**. We anticipate that complexes **1** and **2** can be successfully reduced to the remarkable cationic complex $[Cu(odppf)_2]^{+}$, **3** ,which, although exceedingly reactive toward dioxygen, turns out to be quite stable toward valence disproportionation in aprotic solvents.

Despite the large number of adducts of copper(II) halides and carboxylates with phosphine oxides reported so far,[3] homoleptic

† Dipartimento di Chimica Inorganica, Metallorganica e Analitica, Università di Padova.

‡ Dipartimento di Chimica Organica, Università di Padova.

§ Dipartimento di Chimica Fisica, Università di Padova.

|| Centro di Ricerca sulla Stabilità e Reattività dei Composti di Coordinazione.

⊥ Università de L'Aquila.

⊗ Abstract published in *Advance ACS Abstracts,* October 15, 1995.

(1) Pilloni, G.; Corain, B.; Degano, M.; Longato, B.; Zanotti, G. *J. Chem. Soc., Dalton Trans.* **1993**, 1777.

(2) (a) Clemente, D. A.; Pilloni, G.; Corain, B.; Longato, B.; Tiripicchio-Camellini, M. *Inorg. Chim. Acta* **1986**, *115*, L9. (b) Longato, B.; Pilloni, G.; Bonora, G. M.; Corain, B. *J. Chem. Soc., Chem. Commun.* **1986**, 1478. (c) Longato, B.; Corain, B.; Bonora, G. M.; Pilloni, G. *Inorg. Chim. Acta* **1987**, *137*, 75. (d) Casellato, U.; Ajò, D.; Valle, G.; Corain, B.; Longato, B.; Graziani, R. *J. Crystallogr. Spectrosc. Res.* **1988**, *18*, 593. (e) Longato, B.; Pilloni, G.; Valle, G.; Corain, B. *Inorg. Chem.* **1988**, *27*, 956. (f) Scarcia, V.; Furlani, A.; Longato, B.; Corain, B.; Pilloni, G. *Inorg. Chim. Acta* **1988**, *153*, 67. (g) Corain, B.; Longato, B.; Favero, G.; Ajò, D.; Pilloni, G.; Russo, U.; Kreissl, F. R. *Inorg. Chim. Acta* **1989**, *157*, 259. (h) Casellato, U.; Corain, B.; Graziani, R.; Longato, B.; Pilloni, G. *Inorg. Chem.* **1990**, *29*, 1193. (i) Longato, B.; Pilloni, G.; Graziani, R.; Casellato, U. *J. Organomet. Chem.* **1991**, *404*, 369. (j) Pilloni, G.; Graziani, R.; Longato, B.; Corain, B. *Inorg. Chim. Acta* **1991**, *190*, 165. (k) Pilloni, G.; Longato, B.; Corain, B. *J. Organomet. Chem.* **1991**, *420*, 57; (l) Casellato, U.; Graziani, R.; Pilloni, G. *J. Crystallogr. Spectrosc. Res.* **1993**, *23*, 571. (m) Pilloni, G.; Longato, B. *Inorg. Chim. Acta* **1993**, *208*, 17.

0020-1669/95/1334-5910$09.00/0

phosphine oxide complexes of copper(II) are relatively rare, and tetrahedral, square-planar, and square-pyramidal as well as octahedral structures have been assigned by means of X-ray powder diffraction studies and mostly on the bases of reflectance and IR spectra.[4] To the best of our knowledge, only one of these species have been characterized by single-crystal X-ray analysis.[4m]

This work is aimed also to contributing to the evaluation of the ability of $\{O_4\}$ ligand sets to stabilize the Cu^I state *vs* the Cu^{II} one.

Experimental Section

General Procedures and Materials. All reactions and manipulations of solutions were performed under a nitrogen atmosphere. Anhydrous 1,2-dichloroethane, DCE, and 1,1′-bis(diphenylphosphino)-ferrocene, dppf, were purchased from Aldrich, absolute ethanol from C. Erba and were used as received. Electrochemical grade tetrabutylammonium hexafluorophosphate, TBAH, was obtained from Fluka and used without further purification after drying in vacuo at 60 °C. Commercially available copper(II) tetrafluoroborate (Aldrich) was crystallized twice from dilute aqueous HBF_4 by cooling from room temperature in polyethylene vessels. All other reagents and starting materials were of reagent-grade quality and were used as supplied. High purity argon, further purified from oxygen by passage over reduced copper at 450 °C, was used in the electrochemical experiments.

Synthesis of Complexes. The ligand 1,1′- bis(oxodiphenylphosphoranyl)ferrocene, odppf, was prepared as previously reported.[2k]

$[Cu(odppf)_2(EtOH)](BF_4)_2$ (1). A solution of $[Cu(OH_2)_6](BF_4)_2$ (0.88 g, 2.55 mmol) in absolute ethanol (5 mL) was added to a solution of odppf (3.0 g, 5.12 mmol) in absolute ethanol (40 mL) at room temperature under nitrogen. The orange solution became brown in color, and within few minutes a buff precipitate was formed. The reaction mixture was stirred for 4 h, and then the solid was recovered by filtration, washed with ethanol, and diethyl ether, and finally dried under vacuum. The solid contained *ca.* one molecule of entrapped ethanol per molecule of complex, as determined by thermal and elemental analyses. The crystallization ethanol molecule could be fully removed in vacuo at 70 °C to give pure **1**, 2.9 g (78%). Anal. Calcd for $C_{70}H_{62}B_2CuF_8Fe_2O_5P_4$: C, 57.74; H, 4.29; Cu, 4.36; Fe, 7.67. Found: C, 57.50; H, 4.26; Cu, 4.30; Fe, 7.75. IR (Nujol, ν/cm^{-1}): 3520 w [O−H]; 1155 *vs*, br, [P═O]; 1070 s, br and composite owing to odppf bands [B−F].

$[Cu(odppf)_2](BF_4)_2$ (2). Dissolution of **1** (0.50 g, 0.34 mmol) in anhydrous dichloroethane (5 mL) gave a brown-green solution, and reprecipitation with *n*-hexane (10 mL) at room temperature gave a pea green precipitate, which was filtered off, washed with *n*-hexane, and carefully dried under vacuum. The yield was essentially quantitative. Anal. Calcd for $C_{68}H_{56}B_2CuF_8Fe_2O_4P_4$: C, 57.93; H, 4.00. Found: C, 57.40; H, 4.10. Molar conductivity in nitromethane (1.00 mmol dm^{-3}): Λ_M = 172 Ω^{-1} cm^2 mol^{-1}. IR (Nujol, ν/cm^{-1}): 1128 *vs* [P═O]; 1080 s, br, and composite owing to odppf bands [B-F]. IR (DCE soln, ν/cm^{-1}): 1128 *vs* [P═O].

For comparison, the IR spectrum of the uncoordinated odppf ligand displays a strong ν(P═O) absorption at 1168 cm^{-1} in Nujol mull[5] and a single ν(P═O) band at 1169 cm^{-1} in DCE solution. Also, the copper(I) complex $[Cu(dppf)(odppf)](BF_4)$[1] exhibits a strong ν(P═O) absorption at 1166 cm^{-1} in Nujol mull and 1161 cm^{-1} in DCE solution.

Apparatus and Procedure. The solid state and solution IR spectra were obtained using a Nicolet 5SXC-FTIR spectrometer. Electronic spectra were recorded on a Varian Cary 5/E spectrophotometer. ^{31}P NMR spectra were recorded on a Jeol 90 Q spectrometer equipped with a variable-temperature apparatus and were referenced to external H_3PO_4 (85% w/w). X-band ESR experiments were carried out using a computer-controlled Bruker ER 200 D spectrometer. ESR computer simulations were performed with the program RIGID written by G. Lozos, B. Hoffman, C. Franz, Chemistry Department, Northwestern University. The program assumed coincident **g** and **A** tensor principal axes. All electrochemical experiments were performed in anhydrous deoxygenated DCE solutions with 0.2 mol dm^{-3} TBAH as the supporting electrolyte, using a conventional three-electrode liquid-jacketed cell. Cyclic voltammetry (CV) measurements were performed with an Amel 551 potentiostat modulated by an Amel 566 function generator, and the recording device was an Amel model 863 X-Y recorder. The working electrode was a planar glassy-carbon electrode (*ca.* 2 mm^2) surrounded by a platinum spiral counter electrode. Controlled-potential electrolyses were performed with an Amel 552 potentiostat linked to an Amel 731 digital integrator. The working electrode was a glassy-carbon sheet (*ca.* 40 cm^2), and the counter electrode was external, the connection being made through an appropriate salt bridge. In all cases silver/0.1 mol dm^{-3} silver perchlorate in AN, separated from the test solution by 0.2 mol dm^{-3} TBAH in DCE solution sandwiched between two fritted disks, was used as the reference electrode. Compensation for *iR* drop was achieved by positive feedback. Ferrocene was added at the end of each experiment as the internal reference. All potentials are referred to the ferrocenium/ferrocene redox couple ($E_{1/2}$ = + 0.120 V relative to the actual Ag/$AgClO_4$ reference electrode and +0.420 V *vs* aqueous SCE under the present experimental conditions).

X-ray Crystallography

Suitable crystals of **1**, analyzing as $[Cu(odppf)_2(EtOH)](BF_4)_2 \cdot EtOH$, were obtained by slow evaporation in a refrigerator of a dichloromethane/ethanol solution. Single crystals of **2**, analyzing as $[Cu(odppf)_2](BF_4)_2 \cdot 2CH_3NO_2$, were grown by slow diffusion of toluene (by layering) into a nitromethane solution of the complex. The intensities of the diffracted beam were measured at room temperature on a Philips PW 1100 four-circle automated diffractometer with Mo Kα (λ = 0.710 70 Å) and a graphite monochromator in the incident beam. Unit cell dimensions were obtained from a least-squares fit on the setting angle for 25 reflections (14° < 2θ < 24°). Data were collected by the $\theta-2\theta$ scan technique, and the intensities (±10%) of three reflections were monitored every 50 reflections. The data were corrected for Lorentz−polarization effects, and no absorption was considered. The structure was solved by the SHELXS 86 direct method,[6a] and the refinement was performed by standard full-matrix least-squares using SHELX 76 program.[6b] For both complexes all non-hydrogen atoms, except those of EtOH and CH_3NO_2 molecules and of BF_4^- anions, were allowed to vibrate anisotropically, and H atoms included in ideal position. The phenyl and cyclopentadienyl rings were refined as rigid bodies, with C−C and C−H distances fixed at 139.5

(3) See for example: (a) Lobana, T. S. In *The Chemistry of Organophosphorus Compounds*; Hartley, F. R., Ed; Wiley-Interscience: Chichester, England, 1992; Vol. 2, Chapter 8, pp 434−437 and 462 and references therein. (b) McDonald, R. G.; Hitchman, M. A. *Inorg. Chem.* **1990**, *29*, 3081. (c) Jin, D.; Yang, R.; Xue, B.; Kozawa, K.; Uchida, T. *J. Coord. Chem.* **1992**, *26*, 321. (d) Godfrey, S. M.; McAuliffe, C. A.; Ranger, G. C.; Kelly, D. G. *J. Chem. Soc., Dalton Trans.* **1993**, 2809. (e) Yang, R.; Xue, B.; Jin, D. *Haxue Xuebao* **1993**, *51*, 983; *Chem. Abstr.* **1994**, *120*, 181645d.

(4) (a) Bannister, E.; Cotton, F. A. *J. Chem. Soc.* **1960**, 1878. (b) Cotton, F. A.; Barnes, R. D.; Bannister, E. *J. Chem. Soc.* **1960**, 2199. (c) Hunter, S. H.; Nyholm, R. S.; Rodley, G. A. *Inorg. Chim. Acta* **1969**, *3*, 631. (d) Karayannis, N. M.; Mikulski, C. M.; Pytlewski, L. L.; Labes, M. M. *Inorg. Chem.* **1970**, *9*, 582. (e) Karayannis, N. M.; Mikulski, C. M.; Strocko, M. J.; Pytlewski, L. L.; Labes, M. M. *J. Inorg. Nucl. Chem.* **1971**, *33*, 2691. (f) DeBolster, M. W. G.; Kortram, I. E.; Groeneveld, W. L. *J. Inorg. Nucl. Chem.* **1972**, *34*, 575. (g) Brisdon, B. J. *J. Chem. Soc., Dalton Trans.* **1972**, 2247. (h) Sandhu, S. S.; Sandhu, R. S. *Indian J. Chem.* **1975**, *13*, 390; *C. A.* **1975**, *83*, 52588f. (i) DeBolster, M. W. G.; Boutkan, C.; Van der Knaap, T. A.; Van Zweeden, L.; Kortram, I. E.; Groeneveld, W. L. *Z. Anorg. Allg. Chem.* **1978**, *443*, 269. (j) Kabachnik, M. I.; Sinyavskaya, E. I.; Tsymbal, L. V.; Medved, T. Ya.; Polikarpov, Yu.M.; Bodrin, G. V. *Zh. Neorg. Khim.* **1982**, *27*, 311; *C. A.* **1983**, *98*, 118463e. (k) Planinic, P. B.; Meider, H. *Polyhedron* **1983**, *2*, 69. (l) Sinyavskaya, E. I. *Zh. Neorg. Khim.* **1983**, *28*, 2026; *Chem. Abstr.* **1983**, *99*, 151046q. (m) Yatsimirskii, K. B.; Struchkov, Yu.T.; Batsanov, A. S.; Sinyavskaya, E. I. *Koord. Khim.* **1985**, *11*, 826; *Chem. Abstr.* **1985**, *103*, 79852f.

(5) Bishop, J. J.; Dasison, A.; Katcher, M. L.; Lichtenberg, D. W.; Merrill, R. E.; Smart, J. S. *J. Organomet. Chem.* **1971**, *27*, 241.

(6) (a) Sheldrick, G. M. *SHELXS 86, Program for Crystal Structure Determination*; University of Göttingen: Göttingen, Germany, 1986. (b) Sheldrick, G. M. *SHELX 76, Program for Crystal Structure Solution and Refinement*; Cambridge University: Cambridge, England, 1976.

Table 1. Crystallographic Data for the Complexes $[Cu(odppf)_2(C_2H_5OH)](BF_4)_2$, **1**, and $[Cu(odppf)_2](BF_4)_2$, **2**[a]

complex	$[Cu(odppf)_2(EtOH)]$-$(BF_4)_2$·EtOH (**1**·EtOH)	$[Cu(odppf)_2]$-$(BF_4)_2$·$2CH_3NO_2$ (**2**·$2CH_3NO_2$)
formula	$C_{72}H_{68}B_2$-$CuF_8Fe_2O_6P_4$	$C_{70}H_{62}N_2B_2$-$CuF_8Fe_2O_8P_4$
cryst color	orange	dark-green
MW	1502.08	1532.02
a/Å	19.484(2)	12.325(2)
b/Å	13.450(2)	33.137(3)
c/Å	25.477(2)	17.608(2)
β/deg	93.9(1)	108.7(2)
V/Å^3	6661(2)	6812(8)
Z	4	4
F(000)	3084	3132
D_{calcd}/g cm^{-3}	1.50	1.49
μ/cm^{-1}	4.15	4.10
2*θ* limit/deg	56	50
no. of obsd reflcns	4523	7690
no. of reflctns with $F_o^2 > 3\sigma(F_o^2)$	4162	4778
no. of variables	637	589
R[b]	0.059	0.090
R_w[c]	0.062	0.090
goodness of fit[d]	0.988	6.8[e]

[a] Details in common: monoclinic system, space group $P2_1/c$ (No. 14); graphite monochromatic Mo−Kα radiation (λ = 0.710 70 Å); temperature 21 °C. [b] $R = \sum[|F_o| - |F_c|/\sum|F_o|]$. [c] $w(\mathbf{1}) = 1/[\sigma^2(F) + 0.002(F)^2]$; $w(\mathbf{2}) = 1$. [d] GOF = $[\sum w(|F_o| - |F_c|)^2/(NO - NV)]^{1/2}$, where NO is the number of observations and NV is the number of variables. [e] Meaningless owing to the forced use of $w = 1$.

and 108 pm. All hydrogen atoms were calculated and not refined. The scattering factor for all atoms was taken from ref 7 . Crystal data and final traditional *R* factors are reported in Table 1. Fractional atomic coordinates are listed in Tables 2 and 3. Complete lists of atomic coordinates, thermal parameters, bond lengths and angles, and structure factors have been deposited and are available from the Cambridge Crystallographic Data Centre.

Results and Discussion

Solution State Analysis of the Complexes. The presence in **1** of a weakly coordinated ethanol molecule and the consequent occurrence of a facile and reversible equilibrium between **1** and **2** in noncoordinating solvents were first established by visible and FTIR spectrophotometries. In the 360−1000 nm spectral region both complexes **1** and **2** exhibit in DCE solution a easily detectable band at 450 nm (ϵ = 450 M^{-1} cm^{-1}), attributable to an e_{2g}−e_{1g} transition in the ferrocenyl moiety by analogy with the 441 nm band of ferrocene. This absorption band is energetically identical to that exhibited by odppf, the relevant ϵ being twice as large as that in the uncoordinated organometallic chromophore (λ_{max} = 441 nm; ϵ = 200 M^{-1} cm^{-1}). In addition to this feature, both **1** and **2** display a ligand field band at 855 nm (ϵ = 180 M^{-1} cm^{-1}). Upon stepwise addition of increasing amounts of ethanol to the DCE solution of either **1** or **2**, the greenish color changes gradually to orange and the 855-nm absorption loses concomitantly intensity, while the 450-nm ferrocenyl band remains unchanged. Control experiments reveal that in pure ethanol the 855-nm signal is still present, but the absorption maximum has shifted toward lower wavenumbers (λ = 875 nm), losing most of the intensity ($\epsilon \cong$ 40 M^{-1} cm^{-1}). The data obtained from experiments in which spectra were recorded as a function of added ethanol concentration are consistent with the occurrence

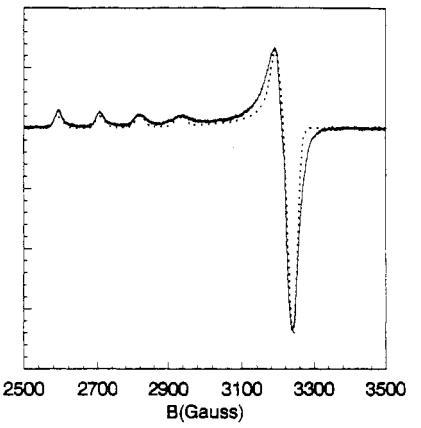

Figure 1. ESR spectrum of **1** in ethanol at 100 K. Key: solid line, experimental; dashed line, simulated.

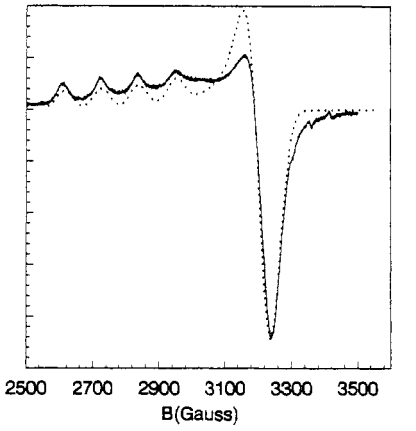

Figure 2. ESR spectrum of **2** in dichloroethane at 100 K. Key: solid line, experimental; dashed line, simulated).

of the tetra−penta coordination equilibrium (1).

$$[Cu(odppf)_2]^{2+} + EtOH \rightleftarrows [Cu(odppf)_2(EtOH)]^{2+} \quad (1)$$

An excellent fit was found for $K = 0.90 \pm 0.05$ dm^3 mol^{-1} (11.7 ± 0.7 molar fraction units) in DCE at 25 °C. The absence of competing anion coordination is inferred by conductivity measurements in nitromethane solution, from the molar conductivity of **2** being in agreement with those expected for a 2:1 electrolyte,[8] and by the lack of splitting of the ν(B−F) in solid **1** and **2** (see Experimental Section).

The release of 1 mol of ethanol per mole of complex upon dissolving **1** in noncoordinating solvents has been confirmed by FTIR on the filtrate after addition of *n*-hexane (see Experimental Section). Thus, IR spectra of these solutions are characterized by two bands at 3613 and 1051 cm^{-1} typical of O−H and C−O stretching vibrations of ethanol, respectively. Calibration curves in the same solvent mixture made possible the quantitative evaluation of released ethanol.

Electron Spin Resonance Spectra. Frozen solutions of **1** in ethanol and of **2** in DCE have been examined by ESR spectroscopy. The 100 K corresponding spectra are reported in Figures 1 and 2.

It appears that the spectra are rather similar, showing the typical features of axial symmetric Cu^{II} complexes.[9] The spectrum of **1** can be computer simulated with the following spin hamiltonian parameters: $g_z = 2.431$, $g_x = g_y = 2.086$; A_z = 114 G, $A_x = A_y = 8$ G, where g_i are the **g** tensor components

(7) *International Tables for X-Ray Crystallography*; Kynoch Press: Birmingham, England, 1974, vol. 4.

(8) Geary, W. J. *Coord. Chem. Rev.* **1971**, *7*, 81 and references therein.

(9) Wertz, J. E.; Bolton, J. R. *Electron Spin Resonance. Elementary Theory and Practical Applications*; McGraw-Hill: New York, 1972.

Table 2. Fractional Coordinates with Isotropic (Denoted by an Asterisk) or Equivalent Isotropic Thermal Parameters (Å^2) for **1**·EtOH

atom	*x*	*y*	*z*	$U_{is/eq}$[a]	atom	*x*	*y*	*z*	$U_{is/eq}$[a]
Cu	0.70918(6)	0.2537(1)	0.19443(5)	0.0375(5)	C(38)	0.9647(3)	0.5337(6)	0.0611(3)	0.090(7)
Fe(1)	0.80340(8)	0.5684(1)	0.25029(7)	0.0440(6)	C(39)	0.9574(3)	0.4491(6)	0.0919(3)	0.086(7)
Fe(2)	0.85050(7)	0.0320(1)	0.09710(6)	0.0356(6)	C(40)	0.8945(3)	0.4286(6)	0.1127(3)	0.059(5)
P(1)	0.8356(1)	0.0825(2)	0.2252(1)	0.036(1)	C(41)	0.6916(4)	0.4858(7)	0.0826(3)	0.054(5)
P(2)	0.7554(1)	0.3608(2)	0.3129(1)	0.040(1)	C(42)	0.6324(4)	0.5391(7)	0.0924(3)	0.075(6)
P(3)	0.7599(2)	0.4697(2)	0.1329(1)	0.043(1)	C(43)	0.5810(4)	0.5532(7)	0.0522(3)	0.113(8)
P(4)	0.6831(1)	0.1172(2)	0.0872(1)	0.038(1)	C(44)	0.5889(4)	0.5141(7)	0.0023(3)	0.13(1)
O(1)	0.7742(3)	0.1407(5)	0.2053(3)	0.046(3)	C(45)	0.6481(4)	0.4608(7)	−0.0075(3)	0.12(1)
O(2)	0.7300(4)	0.3030(5)	0.2661(3)	0.051(3)	C(46)	0.6995(4)	0.4466(7)	0.0327(3)	0.082(6)
O(3)	0.7593(4)	0.3675(5)	0.1575(3)	0.052(3)	C(47)	0.7518(4)	0.5671(5)	0.1793(3)	0.042(4)
O(4)	0.6769(3)	0.1994(5)	0.1269(3)	0.044(3)	C(48)	0.7044(4)	0.5652(5)	0.2192(3)	0.050(5)
O(5)	0.6094(4)	0.2731(8)	0.2093(3)	0.098(4)	C(49)	0.7144(4)	0.6527(5)	0.2500(3)	0.063(6)
C(1)	0.8145(4)	0.0000(5)	0.2762(3)	0.039(4)	C(50)	0.7680(4)	0.7086(5)	0.2291(3)	0.068(6)
C(2)	0.8644(4)	−0.0581(5)	0.3034(3)	0.049(5)	C(51)	0.7912(4)	0.6557(5)	0.1854(3)	0.054(5)
C(3)	0.8453(4)	−0.1267(5)	0.3407(3)	0.071(6)	C(52)	0.8185(4)	0.4504(6)	0.2992(3)	0.042(5)
C(4)	0.7763(4)	−0.1373(5)	0.3509(3)	0.080(7)	C(53)	0.8341(4)	0.5398(6)	0.3273(3)	0.053(5)
C(5)	0.7263(4)	−0.0792(5)	0.3237(3)	0.074(6)	C(54)	0.8882(4)	0.5884(6)	0.3027(3)	0.070(6)
C(6)	0.7454(4)	−0.0106(5)	0.2864(3)	0.057(5)	C(55)	0.9060(4)	0.5291(6)	0.2596(3)	0.064(6)
C(7)	0.6574(4)	0.0002(5)	0.1113(3)	0.040(4)	C(56)	0.8629(4)	0.4439(6)	0.2574(3)	0.051(5)
C(8)	0.6315(4)	−0.0046(5)	0.1610(3)	0.050(5)	C(57)	0.7938(4)	0.2802(6)	0.3626(3)	0.043(4)
C(9)	0.6127(4)	−0.0961(5)	0.1814(3)	0.071(6)	C(58)	0.8531(4)	0.3070(6)	0.3931(3)	0.061(5)
C(10)	0.6198(4)	−0.1828(5)	0.1522(3)	0.071(6)	C(59)	0.8810(4)	0.2422(6)	0.4317(3)	0.068(5)
C(11)	0.6456(4)	−0.1780(5)	0.1026(3)	0.062(6)	C(60)	0.8497(4)	0.1508(6)	0.4397(3)	0.072(6)
C(12)	0.6644(4)	−0.0865(5)	0.0821(3)	0.049(5)	C(61)	0.7904(4)	0.1241(6)	0.4092(3)	0.072(6)
C(13)	0.9294(3)	0.0008(5)	0.1506(3)	0.041(4)	C(62)	0.7624(4)	0.1888(6)	0.3707(3)	0.053(5)
C(14)	0.8659(3)	0.0023(5)	0.1749(3)	0.034(4)	C(63)	0.6882(4)	0.4257(6)	0.3423(3)	0.046(5)
C(15)	0.8224(3)	−0.0711(5)	0.1502(3)	0.035(4)	C(64)	0.6246(4)	0.4391(6)	0.3146(3)	0.054(5)
C(16)	0.8589(3)	−0.1180(5)	0.1107(3)	0.047(5)	C(65)	0.5750(4)	0.4998(6)	0.3351(3)	0.085(7)
C(17)	0.9250(3)	−0.0736(5)	0.1109(3)	0.046(5)	C(66)	0.5889(4)	0.5471(6)	0.3834(3)	0.104(8)
C(18)	0.7684(3)	0.1080(6)	0.0654(3)	0.039(4)	C(67)	0.6525(4)	0.5337(6)	0.4111(3)	0.090(7)
C(19)	0.8208(3)	0.1762(6)	0.0827(3)	0.040(4)	C(68)	0.7021(4)	0.4730(6)	0.3906(3)	0.069(6)
C(20)	0.8801(3)	0.1552(6)	0.0551(3)	0.044(5)	C(69)	0.546(1)	0.291(2)	0.1688(9)	0.200000*
C(21)	0.8643(3)	0.0740(6)	0.0208(3)	0.055(5)	C(70)	0.485(2)	0.304(3)	0.195(1)	0.200000*
C(22)	0.7953(3)	0.0448(6)	0.0271(3)	0.040(4)	O(6)	0.7443(9)	0.723(2)	0.4952(7)	0.200000*
C(23)	0.6282(4)	0.1430(6)	0.0295(3)	0.042(4)	C(71)	0.710(2)	0.811(3)	0.479(2)	0.200000*
C(24)	0.5590(4)	0.1160(6)	0.0286(3)	0.072(6)	C(72)	0.656(2)	0.782(2)	0.444(1)	0.200000*
C(25)	0.5143(4)	0.1413(6)	−0.0145(3)	0.083(7)	B(1)	0.075(1)	0.322(2)	0.553(1)	0.129(8)*
C(26)	0.5388(4)	0.1936(6)	−0.0566(3)	0.074(6)	F(1)	0.0617(5)	0.4294(8)	0.5656(4)	0.142(4)*
C(27)	0.6080(4)	0.2206(6)	−0.0557(3)	0.075(6)	F(2)	0.0436(5)	0.3145(7)	0.5056(4)	0.124(3)*
C(28)	0.6527(4)	0.1953(6)	−0.0127(3)	0.062(5)	F(3)	0.0455(4)	0.2788(6)	0.5919(3)	0.111(3)*
C(29)	0.9073(3)	0.1600(5)	0.2473(3)	0.041(4)	F(4)	0.1418(6)	0.3210(8)	0.5572(4)	0.158(4)*
C(30)	0.9316(3)	0.1666(5)	0.3000(3)	0.047(5)	B(2)	0.549450	0.397160	0.827120	0.20(1)*
C(31)	0.9877(3)	0.2275(5)	0.3144(3)	0.060(6)	F(5)	0.480950	0.394860	0.804640	0.200000*
C(32)	1.0195(3)	0.2818(5)	0.2762(3)	0.055(5)	F(6)	0.558930	0.455110	0.778520	0.200000*
C(33)	0.9952(3)	0.2752(5)	0.2236(3)	0.051(5)	F(7)	0.588230	0.450680	0.863420	0.200000*
C(34)	0.9391(3)	0.2143(5)	0.2091(3)	0.048(5)	F(8)	0.590120	0.314870	0.812670	0.200000*
C(35)	0.8389(3)	0.4927(6)	0.1026(3)	0.037(4)	F(5)′	0.485430	0.375090	0.836190	0.200000*
C(36)	0.8462(3)	0.5773(6)	0.0718(3)	0.065(5)	F(7)′	0.568290	0.416290	0.876400	0.200000*
C(37)	0.9091(3)	0.5978(6)	0.0511(3)	0.084(7)	F(8)′	0.550280	0.296530	0.811540	0.200000*

[a] U_{eq} is defined as one-third of the trace of the orthogonalized U_{ij} tensor.

along and perpendicular to the symmetry axis *z*, and A_i the tensor components of the hyperfine interaction of the unpaired electron with the copper nucleus. The spin Hamiltonian parameters obtained by the computer simulation for complex **2** are: g_z = 2.415, $g_x = g_y$ = 2.095; A_z = 112 G, $A_x = A_y$ = 10 G. The similarity between the *g* and *A* values exhibited by **1** and **2** indicates that in solution the two complexes should have a related structure. The **g** tensor values for the tetracoordinated complex **2** fit with the occupation of the $d_{x^2-y^2}$ orbital by the unpaired electron, as expected in a square-planar molecular geometry. The *g* value pattern for five-coordinate complex **1** is also indicative of a $d_{x^2-y^2}$ ground state and points unambiguously to a square-pyramidal geometry around the copper atom. In fact, a trigonal-bipyramidal structure would have given **g** tensor components in the reverse order, *i.e.* a lower value, equal to the free electron g_e value, for the *z* component and larger figures for the *x* and *y* directions.

Apparently, for complex **2** the square-planar geometry is maintained in the solid state, while complex **1** appears to adopt a trigonal-bipyramidal structure in the crystal lattice (*see* next section). Solid state packing forces are likely responsible for the observed behavior as this *tbp*−*spy* configurational change is not surprising in light of the small energy difference known to characterize the two geometries.[10]

As pointed out above, for both **1** and **2** the g_z value turns out to be remarkably high, when compared with the typical figures referring to {CuO_4} chromophores. In particular, it appears clearly that g_z for **2** differs from those of square-planar complexes in which the copper−oxygen bond is largely covalent in character and the unpaired electron is significantly delocalized on the relevant ligands.[11] On the contrary, the g_z value nicely agrees with those observed for {CuO_6} chromophores occurring in ionic compounds, for which the unpaired electron is believed

(10) Cotton, F. A.; Wilkinson, G. *Advanced Inorganic Chemistry*, 5th ed.; Wiley: New York, 1988; p 13.

(11) (a) McGarvey, B. R. *J. Phys. Chem.*, **1956**, *60*, 71. (b) Gersmann, H. R.; Swalen, J. D. *J. Chem. Phys.* **1962**, *36*, 3221. (c) Hathaway, B. J.; Billing, D. E.; Dudley, R. J. *J. Chem. Soc. A* **1970**, 1420.

Table 3. Fractional Coordinates with Isotropic (Denoted by an Asterisk) or Equivalent Isotropic Thermal Parameters (Å^2) for **2**·2CH_3NO_2

atom	*x*	*y*	*z*	$U_{is/eq}$[a]	atom	*x*	*y*	*z*	$U_{is/eq}$[a]
Cu	0.3967(1)	0.61915(6)	0.7508(1)	0.0391(7)	C(40)	0.4387(8)	0.6545(4)	0.5170(7)	0.053(7)
Fe(1)	0.4010(2)	0.50326(7)	0.7705(1)	0.0434(8)	C(41)	0.3627(8)	0.6685(3)	0.9763(6)	0.047(7)
Fe(2)	0.4037(2)	0.73411(7)	0.7413(1)	0.0457(9)	C(42)	0.2519(8)	0.6836(3)	0.9596(6)	0.059(8)
P(1)	0.4362(3)	0.6743(1)	0.9050(2)	0.039(1)	C(43)	0.1922(8)	0.6776(3)	1.0138(6)	0.08(1)
P(2)	0.1736(3)	0.5673(1)	0.7308(2)	0.043(2)	C(44)	0.2432(8)	0.6564(3)	1.0848(6)	0.08(1)
P(3)	0.6236(3)	0.5669(1)	0.7883(2)	0.044(2)	C(45)	0.3540(8)	0.6413(3)	1.1015(6)	0.08(1)
P(4)	0.3639(3)	0.6654(1)	0.5877(2)	0.043(1)	C(46)	0.4138(8)	0.6473(3)	1.0472(6)	0.063(8)
O(1)	0.4354(8)	0.6353(3)	0.8623(5)	0.047(4)	C(47)	0.3662(8)	0.7137(3)	0.8386(6)	0.048(5)
O(2)	0.2413(8)	0.6064(3)	0.7423(6)	0.045(4)	C(48)	0.3957(8)	0.7553(3)	0.8468(6)	0.050(6)
O(3)	0.5526(7)	0.6048(3)	0.7639(6)	0.047(4)	C(49)	0.3151(8)	0.7765(3)	0.7834(6)	0.058(8)
O(4)	0.3596(8)	0.6293(3)	0.6371(5)	0.044(4)	C(50)	0.2359(8)	0.7481(3)	0.7360(6)	0.059(8)
C(1)	0.7556(8)	0.5793(3)	0.8632(5)	0.052(5)	C(51)	0.2674(8)	0.7092(3)	0.7701(6)	0.048(6)
C(2)	0.7725(8)	0.5705(3)	0.9436(5)	0.059(7)	C(52)	0.4154(8)	0.7484(3)	0.6325(5)	0.051(7)
C(3)	0.8715(8)	0.5837(3)	1.0025(5)	0.076(9)	C(53)	0.4368(8)	0.7066(3)	0.6480(5)	0.049(7)
C(4)	0.9538(8)	0.6056(3)	0.9810(5)	0.070(9)	C(54)	0.5336(8)	0.7026(3)	0.7180(5)	0.048(7)
C(5)	0.9370(8)	0.6143(3)	0.9005(5)	0.08(1)	C(55)	0.5720(8)	0.7420(3)	0.7458(5)	0.056(8)
C(6)	0.8379(8)	0.6012(3)	0.8416(5)	0.054(7)	C(56)	0.4989(8)	0.7703(3)	0.6930(5)	0.059(8)
C(7)	0.6520(9)	0.5457(3)	0.7037(5)	0.057(7)	C(57)	0.0402(7)	0.5737(3)	0.6541(6)	0.041(6)
C(8)	0.5849(9)	0.5576(3)	0.6271(5)	0.059(7)	C(58)	-0.0326(7)	0.6042(3)	0.6635(6)	0.070(8)
C(9)	0.5970(9)	0.5384(3)	0.5598(5)	0.08(1)	C(59)	-0.1376(7)	0.6106(3)	0.6042(6)	0.08(1)
C(10)	0.6762(9)	0.5072(3)	0.5691(5)	0.08(1)	C(60)	-0.1700(7)	0.5866(3)	0.5355(6)	0.09(1)
C(11)	0.7433(9)	0.4952(3)	0.6458(5)	0.09(1)	C(61)	-0.0972(7)	0.5561(3)	0.5262(6)	0.12(1)
C(12)	0.7312(9)	0.5145(3)	0.7130(5)	0.068(9)	C(62)	0.0079(7)	0.5497(3)	0.5855(6)	0.085(9)
C(13)	0.5554(8)	0.5292(3)	0.8297(6)	0.041(6)	C(63)	0.0645(8)	0.5234(3)	0.8190(6)	0.064(6)
C(14)	0.5685(8)	0.4867(3)	0.8262(6)	0.052(7)	C(64)	0.0532(8)	0.5092(3)	0.8907(6)	0.072(9)
C(15)	0.4974(8)	0.4682(3)	0.8657(6)	0.066(8)	C(65)	0.1218(8)	0.5250(3)	0.9637(6)	0.069(9)
C(16)	0.4404(8)	0.4993(3)	0.8936(6)	0.065(8)	C(66)	0.2019(8)	0.5550(3)	0.9651(6)	0.067(9)
C(17)	0.4762(8)	0.5369(3)	0.8714(6)	0.045(6)	C(67)	0.2132(8)	0.5692(3)	0.8934(6)	0.054(6)
C(18)	0.2445(8)	0.5253(3)	0.7034(6)	0.046(6)	C(68)	0.1446(8)	0.5534(3)	0.8204(6)	0.046(5)
C(19)	0.2346(8)	0.4838(3)	0.7207(6)	0.049(6)	B(1)	0.901690	0.718280	0.737050	0.100000*
C(20)	0.3078(8)	0.4615(3)	0.6884(6)	0.054(7)	F(1)	0.995800	0.692280	0.794170	0.150000*
C(21)	0.3630(8)	0.4891(3)	0.6511(6)	0.065(8)	F(2)	0.866350	0.736460	0.782550	0.150000*
C(22)	0.3239(8)	0.5285(3)	0.6604(6)	0.048(7)	F(3)	0.956340	0.739690	0.712270	0.150000*
C(23)	0.5778(7)	0.6912(3)	0.9569(6)	0.048(6)	F(4)	0.820190	0.685890	0.708820	0.150000*
C(24)	0.6669(7)	0.6801(3)	0.9284(6)	0.062(7)	F(4)′	0.837580	0.697720	0.669110	0.150000*
C(25)	0.7762(7)	0.6962(3)	0.9634(6)	0.073(9)	B(2)	0.143210	0.900210	0.737720	0.150000*
C(26)	0.7964(7)	0.7234(3)	1.0269(6)	0.075(9)	F(5)	0.069880	0.872150	0.681770	0.150000*
C(27)	0.7073(7)	0.7344(3)	1.0554(6)	0.067(8)	F(7)	0.167070	0.925250	0.678740	0.150000*
C(28)	0.5980(7)	0.7184(3)	1.0204(6)	0.052(6)	F(8)	0.047110	0.930060	0.729540	0.150000*
C(29)	0.2045(9)	0.7049(4)	0.4615(6)	0.057(7)	F(7)′	0.246320	0.916200	0.737230	0.150000*
C(30)	0.0955(9)	0.7202(4)	0.4222(6)	0.077(9)	F(6)	0.119120	0.914640	0.802640	0.150000*
C(31)	0.0068(9)	0.7138(4)	0.4540(6)	0.08(1)	O(1)A	0.825600	0.422700	0.520900	0.150000*
C(32)	0.0270(9)	0.6920(4)	0.5249(6)	0.08(1)	O(2)A	0.965700	0.456800	0.591800	0.24(1)*
C(33)	0.1359(9)	0.6767(4)	0.5642(6)	0.065(8)	N(1)A	0.925000	0.424500	0.569100	0.23(1)*
C(34)	0.2247(9)	0.6831(4)	0.5325(6)	0.050(7)	C(1)A	0.992500	0.395800	0.605400	0.31(2)*
C(35)	0.3870(8)	0.6303(4)	0.4504(7)	0.073(8)	O(1)B	0.709000	0.877000	0.686400	0.25(2)*
C(36)	0.4430(8)	0.6228(4)	0.3944(7)	0.08(1)	O(2)B	0.732300	0.845200	0.753200	0.30(2)*
C(37)	0.5508(8)	0.6396(4)	0.4051(7)	0.076(9)	N(1)B	0.721000	0.860300	0.719800	0.44(4)*
C(38)	0.6025(8)	0.6637(4)	0.4718(7)	0.072(9)	C(1)B	0.842600	0.840700	0.714800	0.19(1)*
C(39)	0.5464(8)	0.6712(4)	0.5277(7)	0.057(7)					

[a] U_{eq} is defined as one third of the trace of the orthogonalized U_{ij} tensor.

to reside essentially in the metal center, surrounded by an elongated tetragonal−octahedral set of oxide "ligands" (*vide infra*).[12] As a matter of fact, the **g** tensor of a copper complex is determined by the spin−orbit interaction λ ($\lambda_{Cu^{II}} = 830$ cm^{-1}) and by the symmetry of the ligand field acting on the copper ion.[13] In particular, for a square planar geometry one expects $g_z = g_e + 8\lambda/\Delta_1$ and $g_x = g_y = g_e + 2\lambda/\Delta_2$, where Δ_1 is the energy separation between the ground state orbital $d_{x^2-y^2}$ and the d_{xy} orbital, Δ_2 the separation between $d_{x^2-y^2}$ and the degenerate d_{xz} and d_{yz} orbitals. The possible delocalization of the unpaired electron over the ligands is taken into account by reducing the spin−orbit coupling constant according to the fraction of unpaired electron in the copper ion. By assuming for complex **2** $\Delta_1 \cong \Delta_2 = 11\,700$ cm^{-1}, as obtained from the wavelength of the maximum of the broad band in the optical spectrum, the calculated **g** tensor components are $g_z^{calc} = 2.570$ and $g_x^{calc} = g_y^{calc} = 2.144$. A comparison between the calculated and observed **g** tensor parameters clearly indicates that the unpaired electron almost resides in the metal orbital; on the basis of the g^{obs}/g^{calc} figures, the localization can be estimated to be *ca.* 95%. For complex **1**, making allowance for the red shift of the absorption from 855 to 875 nm, the same analysis gives again *ca.* 95% of the unpaired electron in the metal orbital.

Solid-State Structures. The ORTEP drawings of the dication complexes $[Cu(odppf)_2(EtOH)]^{2+}$ and $[Cu(odppf)_2]^{2+}$ of **1** and **2** showing the atom-labeling scheme are depicted in Figures 3 and 4, respectively.

In complex **1** the metal is pentacoordinated with the five donor atoms at the vertices of a distorted trigonal bipyramid formed by two chelated odppf moieties and an ethanol molecule as the fifth ligand (Figure 3). The two oxygen atoms of the odppf ligand occupy an equatorial and an apical position, determining a bite angle in the range 90.1(3)−95.7(3)° . The atoms in the apical positions exibit a Cu−O bond distance (1.946

(12) Van der Pol, A.; Peters, G. M.; Reijerse, E. J.; de Boer, E. *Appl. Magn. Reson.* **1992**, *3*, 751.
(13) McGarvey, B. R. In *Transition Metal Chemistry*; Carlin, R. L., Ed; Dekker: New York, 1966; Vol. 3.

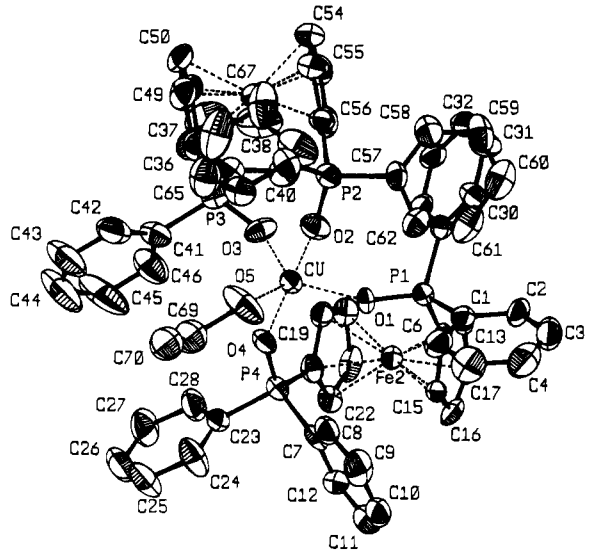

Figure 3. ORTEP drawing of the pentacoordinate $[Cu(odppf)_2(EtOH)]^{2+}$ ion of **1**, showing the atom-labeling scheme. The atoms are shown with 50% probability.

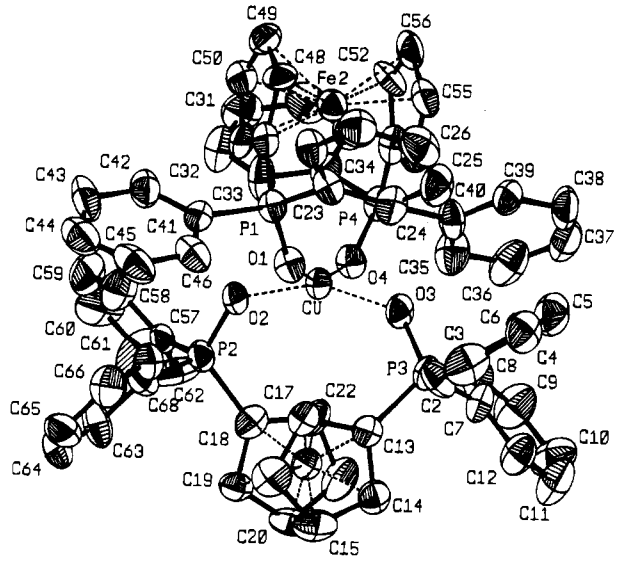

Figure 4. ORTEP drawing of the tetracoordinate $[Cu(odppf)_2]^{2+}$ ion of **2**, showing the atom-labeling scheme. The atoms are shown with 50% probability.

Å , average) significantly shorter than those in the equatorial plane for which the average value of 2.032 Å is observed. The copper atom deviates from the equatorial plane, defined by the atoms O(1), O(3), and O(5), being shifted 0.026(2) Å toward O(2).

The two odppf moieties exhibit significant differences in some structural details: (i) the cyclopentadienyl rings bonded to Fe(1) are virtually parallel (the dihedral angle between the two planes is 0.7(3)° whereas in the other ligand they are tilted toward the metal center, forming a dihedral angle of 4.5(5)°; (ii) the torsion angle of the cyclopentadienyl rings (defined as the angle formed by the lines connecting the Cp carbon atoms bonded to the phosphorus atoms and the centroids of the two Cp rings) is 62.2° in the ligand containing Fe(2) but 75.1° in the other one; (iii) the mean plane containing the atoms O(1), P(1), O(4), and P(4) makes a dihedral angle of 91.2(2)° with the equatorial plane while that formed by the equatorial plane and the mean plane defined by O(2), P(2), O(3), and P(3) is 99.4(3); (iv) the phosphorus atoms P(1) and P(4) deviate *positively*, *i.e.* toward the Fe atom, from the Cp ring planes

Table 4. Selected Bond Distances (Å) and Angles (deg) for $[Cu(odppf)_2(EtOH)](BF_4)_2$·EtOH, **1**·EtOH

Cu−O(1)	1.986(7)	Cu−O(2)	1.960(7)
Cu−O(3)	2.076(7)	Cu−O(4)	1.933(7)
Cu−O(5)	2.023(8)	P(1)−O(1)	1.488(7)
P(2)−O(2)	1.479(8)	P(3)−O(3)	1.511(8)
P(4)−O(4)	1.510(8)	O(5)−C(69)	1.57(3)
O(1)−Cu−O(4)	90.1(3)	O(2)−Cu−O(3)	95.7(3)
O(1)−Cu−O(3)	108.2(4)	O(2)−Cu−O(4)	172.3(4)
O(1)−Cu−O(2)	92.3(3)	O(3)−Cu−O(4)	90.5(3)
O(1)−Cu−O(5)	133.3(4)	O(2)−Cu−O(5)	85.5(4)
O(3)−Cu−O(5)	118.5(4)	O(4)−Cu−O(5)	87.5(4)
Cu−O(1)−P(1)	160.0(5)	Cu−O(2)−P(2)	164.9(5)
Cu−O(3)−P(3)	151.2(7)	Cu−O(4)−P(4)	146.8(5)
O(1)−P(1)−C(14)	111.5(4)	O(2)−P(2)−C(52)	113.4(4)
O(3)−P(3)−C(47)	113.0(4)	O(4)−P(4)−C(18)	112.1(5)
Cu−O(5)−C(69)	128(1)		

Table 5. Selected Bond Distances (Å) and Angles (deg) for $[Cu(odppf)_2](BF_4)_2$·$2CH_3NO_2$, **2**·$2CH_3NO_2$

Cu−O(1)	1.941(9)	Cu−O(2)	1.92(1)
Cu−O(3)	1.92(1)	Cu−O(4)	1.935(9)
P(1)−O(1)	1.49(1)	P(2)−O(2)	1.52(1)
P(3)−O(3)	1.51(1)	P(4)−O(4)	1.49(1)
O(1)−Cu−O(4)	154.0(4)	O(2)−Cu−O(3)	152.8(4)
O(1)−Cu−O(2)	93.2(5)	O(1)−Cu−O(3)	92.0(5)
O(3)−Cu−O(4)	93.6(5)	O(2)−Cu−O(4)	93.4(5)
O(1)−P(1)−C(47)	112.4(6)	O(2)−P(2)−C(18)	113.8(7)
O(3)−P(3)−C(13)	113.0(7)	O(4)−P(4)−C(53)	111.9(5)
Cu−O(1)−P(1)	135.1(6)	Cu−O(2)−P(2)	133.7(8)
Cu−O(3)−P(3)	135.0(8)	Cu−O(4)−P(4)	134.6(6)

(0.0893 and 0.1410 Å , respectively) but P(2) and P(3) deviate *negatively* (−0.064(4) and −0.005(4) Å) from the linked cyclopentadienyl ring.

Finally, it is worth noting that although the coordinated EtOH shows a Cu−O bond distance similar to that of the odppf ligands, the Cu−O(5)−C(69) angle, 128(1)° , is quite different from the values of the Cu−O−P angles which are in the range 151−165° . Such a difference can be explained with the different hybridation of the oxygen atom in the two type of ligands.

The structure of **2** assigned initially on the basis of the spectroscopic data was confirmed by an X-ray crystal structure determination. The crystal structure of **2** reveals that the cationic complex contains monomeric unities in which the coordination geometry around the metal is distorted square-planar where the two odppf moieties act as chelating ligands with bite angles in the range 152.8(4)−154.0(4)°. The remaining O−Cu−O angles approach the value for square-planar geometry being in the range 92.0(5)−93.6(5)°. The Cu−O bond distances fall in the range 1.92(1)−1.941(9) Å (see Table 5) and compare well with the average Cu−O bond length of 1.96 Å in the square-planar $\{CuO_4\}$ grouping in copper(II) oxide.[14]

The Cu−O−P bond angles are in the range 133.7(8)−135.1(6)° whereas the average P−O bond length (1.50 Å) is slightly longer than that of the uncoordinated oxophosphorylic ligand (1.493(2) Å),[1] consistent with the lower P−O stretching frequency observed in the IR spectrum of the complex ($\Delta\nu \cong 40$ cm^{-1}). For the oxophosphorylic unit the observed frequency shifts and bond length adjustments resulting from coordination are generally less than 50 cm^{-1} and 0.01 Å , respectively.[15] The mean planes containing the O(1), P(1), O(4), and P(4) and O(2), P(2), O(3), and P(3) form a dihedral angle of 90.9(4)°. The cyclopentadienyl rings are all planar and slightly tilted toward the Cu center (4.5(5)° for the Cp pertinent to Fe(1) and

(14) Åsbrink, S; Norrby, K. J. *Acta Crystallogr., Sect/ B* **1970**, *26*, 8.
(15) Burford, N. *Coord. Chem. Rev.*, **1992**, *112*, 1 and references therein.

7.2(4)° for those bonded to Fe(2), respectively). The two phosphines exhibit a "synclinal eclipsed" conformation,[16a] being the torsion angle 84.7° for Fe(1) and 82.3° for Fe(2), respectively. The angles O−P−C_{Cp} are not significantly different (111.9(5)−113.8(7)°) from that found in free odppf (111.3(2)°).

In both complexes **1** and **2**, the BF_4^- ions do not interact with the cation. Moreover, bond distances and angles within the two anions exhibit marked differences, thus indicating some disorder in the crystal. The dissimilarity is particularly apparent in complex **2**, and this likely stands among the factors responsible for the relatively high *R* value.

The comparision of the structural data of **2** with those found in the related complex of the copper (I), [Cu(dppf)(odppf)]BF_4, shows that the coordination of two odppf units to the Cu^{II} center causes a remarkable increase of the bite angle (O−Cu−O), from the value 102.1(2)° found in $[Cu(dppf)(odppf)]^+$ to 153° in complex **2**, and a concomitant expected decrease of the Cu−O−P angles, from the values 156−160 to 133−135°.

Electrochemical Results. It is well known that ferrocene-based ligands and their complexes generally exhibit a ferrocene-centered oxidation process. Significant anodic shifts of the redox potential of the ferrocenium/ferrocene couple upon phosphination of the Cp rings and complexation of the resulting dppf ligand as well as variations among the different known coordination modes of the ligand have already been observed in these and other laboratories.[1,2a,e,g,k,m,16]

As expected, the odppf ligand was previously found to undergo an essentially reversible one-electron transfer with a potential value ($E_{1/2}$ = 0.430 V *vs* ferrocenium/ferrocene) more anodic than for the dppf precursor ($E_{1/2}$ = 0.183 V). Moreover, coordination of odppf to the soft Cu^I−dppf moiety produced a further shift of the redox potential to more positive values ($E_{1/2}$ = 0.703 V).[1]

Therefore, it appeared of interest to evaluate how the complexation with the hard Cu^{II} center influenced the redox behavior of the oddf ligand and to check if the presence of two noncommunicating ferrocenyl groups within the metal coordination sphere resulted in either a two-step one-electron or a single step two-electron charge transfer. Figure 5 shows the electrochemical response exhibited by **2** in dichloroethane solution in the anodic portion of the voltage scan.

Thus, **2** undergoes a single two-electron oxidation step with the directly associated, fully developed (i_p^c/i_p^a = 1.0) reduction response in the reverse scan. The redox couple, whose shape and position are independent of scan rate over the range of experimental (20−200 mV s^{-1}) sweep rates, is centered at $E_{1/2}$ = 0.717 V, as the mean value of the potentials for anodic and cathodic peak currents. The occurrence of a two-electron transfer has been verified chronoamperometrically by comparison of the diffusion current with strictly related compounds of known electrochemical behavior[1,2e,m,] and confirmed by controlled-potential coulometry (see above). An inspection of the shape of the voltammetric response clearly indicates that it is slightly sharper than that predicted for a single-stepped two-electron reversible charge transfer reaction involving two noninteracting redox sites in the same molecule under a merely statistical control: the peak to peak separation, ΔE_p, and peak width, $E_p - E_{p/2}$, are 50 and 38 mV rather than 58.5 and 57 mV as expected.[17,18] This figure is attributed to a small negative

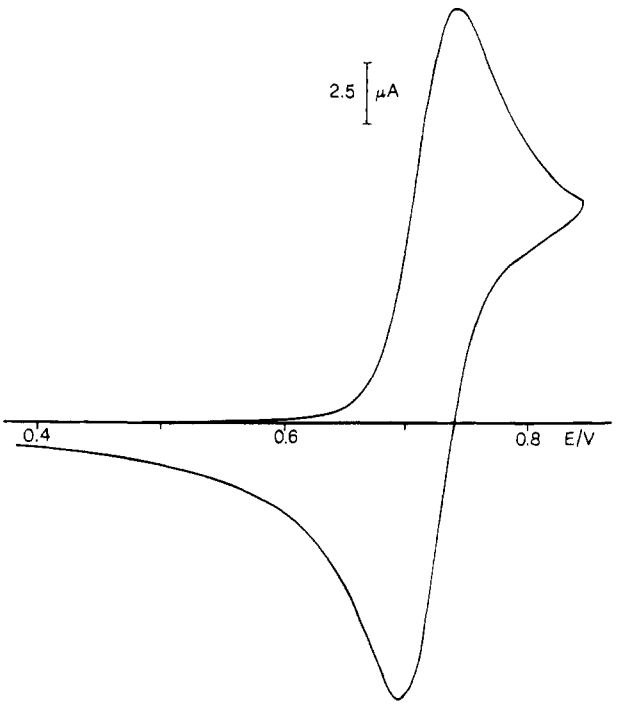

Figure 5. Cyclic voltammogram for oxidation of 3.0 mmol dm^{-3} $[Cu(odppf)_2]^{2+}$ in DCE, 0.2 mol dm^{-3} TBAH, at 25 °C (scan rate 50 mV s^{-1}). Potentials are referred to the ferrocenium/ferrocene couple: $E_{1/2}$ = +0.420 V *vs* aqueous SCE.

difference between the two individual one-electron transfers (E°_1 = 0.732 and E°_2 = 0.717 V, based on the width $E_p - E_{p/2}$[17]) and reveals that electrons are removed almost in a single shot.

Controlled-potential electrolysis carried out at 0 °C and at potentials past the anodic peak results in the exchange of 2 mol of electrons per mole of depolarizer to give an emerald-green solution with a voltammetric reduction profile virtually complementary to the oxidation pattern of the precursor, thus raising in evidence the chemical reversibility of the electron removal. The electronic spectrum of the emerald-green anolyte is reminescent of those observed in the oxidation of complexes containing ferrocenyl-derived ligands[2g,m,19] and in the oxidation of ferrocene itself displaying an absorption band at λ_{max} = 650 ($\epsilon \cong$ 1000 M^{-1} cm^{-1}), which is characteristic of the ferrocenium cation (λ_{max} = 617 nm; ϵ =450 M^{-1} cm^{-1}).[20] Thus, the assignment of the fully oxidation product as the copper(II) complex of the $[odppf]^+$ ligand, $[Cu(odppf)_2]^{4+}$, is substantially supported. However, the spent anolyte is not indefinitely stable: in the long run (hours) the bright green solution turns yellow with contemporary flattening of the voltammetric and spectral signals distinctive of the primary oxidation product. Very likely, this decomposition is promoted by trace amounts of water present in the reaction medium, as suggested by the striking increase of the decomposition rate (within minutes) upon deliberate addition of water. Since the single-electron oxidation product of the uncoordinate ligand, $[oddpf]^+$, is similarly quenched by water,[21] these observations suggest appreciable lability of the fully oxidized complex. At higher temperature, 25 °C, the chemical complication by water keeps up with the progress of the electrolysis so that worthless results are obtained under these conditions.

(16) (a) Gan, K.-S.; Hor, T. S. A. In *Ferrocenes—Homogeneous Catalysis, Organic Synthesis, Materials Science*; Togni, A.; Hayashi, T., Eds; VCH: Weinheim, Germany, 1995; Chapter 1, and references therein. (b) Zanello, P. In ref 16a, Chapter 7, and references therein.
(17) Richardson, D. E.; Taube, H. *Inorg. Chem.* **1981**, *20*, 1278.
(18) Foucher, D. A.; Honeyman, C. H.; Nelson, J. M.; Tang, B. Z.; Manners, I. *Angew. Chem., Int. Ed. Engl.* **1993**, *32*, 1709.
(19) Miller, T. M.; Ahmed, K. J.; Wrighton, M. S. *Inorg. Chem.* **1989**, *28*, 2347.
(20) Sohn, Y. S.; Hendrickson, D. N.; Gray, H. B. *J. Am. Chem. Soc.* **1971**, *93*, 3603.
(21) Pilloni, G.; et al. To be submitted for publication.

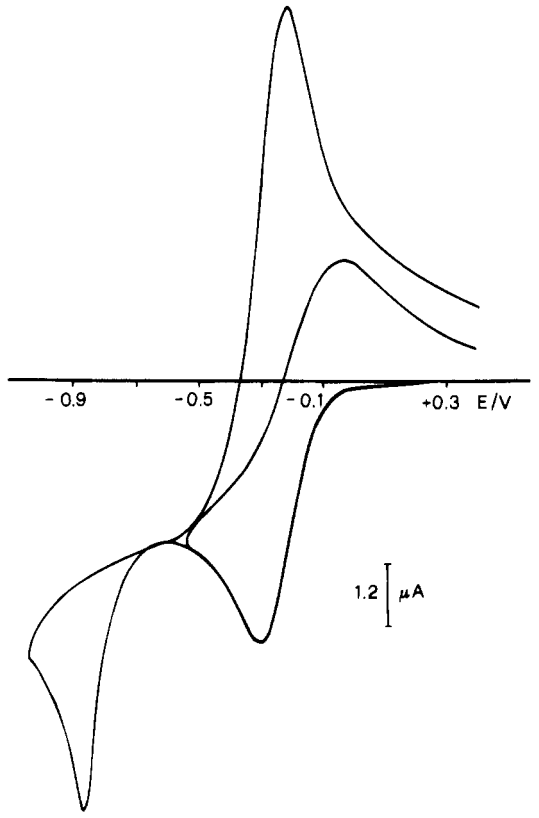

Figure 6. Cyclic voltammogram for reduction of 3.0 mmol dm^{-3} $[Cu(odppf)_2]^{2+}$ in DCE, 0.2 mol dm^{-3} TBAH, at 25 °C (scan rate 50 mV s^{-1}). Potentials are referred to the ferrocenium/ferrocene couple: $E_{1/2}$ = +0.420 V *vs* aqueous SCE.

Particularly interesting is the *reduction pattern* of the title compounds. Figure 6 shows the cyclic voltammogram exhibited by **2** in dichloroethane solution in the cathodic scan of the voltage.

It is apparent that **2** undergoes a chemically reversible reduction centered at $E_{1/2}$ = −0.165 V followed by another reduction process at more negative potential values. Both the processes are electrochemically irreversible, with the second one manifesting evident electrode contamination phenomena (which made it necessary to polish the electrode surface frequently during the experiments) and displaying on the reverse scan a sharp anodic peak at potential values close to those of the first redox couple. Double-potential-step chronoamperometric tests verify that the first reduction is a one-electron transfer (the diffusion current is just half that relevant to the oxidation process described above) and that the reduction product is stable.[22] By the same criteria, the second reduction results to be an overall two-electron transfer without apparent chemical complications. Exhaustive electrolysis at the first process requires one electron/molecule and produces a bright yellow, exceedingly air sensitive solution with a voltammetric profile quite complementary to that shown in Figure 6, thus confirming that the reduction is chemically reversible. The resulting solution is ESR silent and exhibits only the 450-nm ferrocenyl band with unchanged intensity in the electronic spectrum. If the electrolysis is performed at potential values of the second process, an additional 1 mol of electrons per mole of depolarizer is consumed. In the course of the electrolysis the working electrode undergoes an evident coating by metallic copper and the final spent catholyte displays the CV profile characteristic of free odppf ligand, i.e. a redox couple centered at $E_{1/2}$ = 0.430 V. The presence in solution of uncoordinated odppf ligand is confirmed by the 28.24 ppm-resonance in the ^{31}P NMR spectrum.[1]

These results do unambiguously point toward the viability of the homoleptic Cu^I bis(phosphine oxide) complex, possibly the four-coordinate $[Cu(odppf)_2]^+$, **3**, according to the preference exhibited by odppf for binding copper(I) in a bidentate fashion.[1] In fact, the observed sequence of the redox potentials allows one to predict that this species can be generated by either the one-electron reduction of the precursor $[Cu(odppf)_2]^{2+}$ or by the one-electron oxidation of metallic copper in the presence of a 2-fold excess amount of the ligand. The last statement is supported by the successful course of these coulometric tests. As a matter of fact, electrochemical oxidation of a copper foil in DCE containing odppf (1 mol of electrons/2 mol of ligand) produces solutions with electrochemical and chemical features identical with those observed in the one-electron reduction of **2**. Also, the course of the reaction proves to be independent of the applied potential in a wide range of potential values; *i.e.*, the oxidation can be successfully carried out under galvanostatic conditions, thus proving that the comproportionation equilibrium lies to the right in eq 2, favoring **3** in DCE.

$$Cu + 2odppf + [Cu(odppf)_2]^{2+} \rightleftharpoons 2[Cu(odppf)_2]^{+} \quad (2)$$

Control experiments confirm that addition of excess copper turnings to a brown DCE solution of $[Cu(odppf)_2]^{2+}$ and odppf in 1:2 molar ratio causes a gradual equilibration of the mixture to the yellow $[Cu(odppf)_2]^+$ species. This change can be followed by electrochemical and spectrophotometric techniques. Although the identity of **3** remains to be definitely established, tetrahedral CuO_4 coordination is supported by ^{31}P NMR tests on the crude yellow solid recovered from the solution mixture of **2**, odppf, and Cu upon equilibration (see above) and subsequent evaporation of the solvent under reduced pressure. Thus, the CD_2Cl_2 solution $^{31}P\{^1H\}$ spectrum recorded at 36.23 MHz exhibits at room temperature a single broad resonance centered at δ 34.58 ppm which, upon cooling, gradually changes to a sharp signal and moves slightly to higher field. The observed δ value, 33.78 ppm at 183 K, should be compared with those exhibited by the free odppf ligand (28.24 ppm) and by the coordinated one in the closely related complex $[Cu(dppf)(odppf)]^+$ (32.90 ppm), under identical conditions.[1] The temperature dependence of the NMR line shape is consistent with the partial dissociation of one of the Cu−O bonds, which would become significant at room temperature on the NMR time scale. In line with this, the solid-state CPMAS ^{31}P NMR spectrum of crude complex **3** clearly indicates the chemical equivalence of the four phosphorus atoms as well as the absence of any resonance attributable to either uncoordinated or pendant odppf ligand.

In this connection, although the whole of the chemical and electrochemical observations points convincingly to the thermodynamic stability of $[Cu(odppf)_2]^+$, a kinetic barrier to the electron transfer at the electrode surface is apparent ($\alpha \cong 0.5$ from peak width). However, the moderately irreversible character of the relevant electron transfer process can be justified in terms of steric crowding of the bulky odppf ligands and is unlikely to be attributed to the little energetically demanding interconversion of **2** (distorted square-planar) into **3** (essentially tetrahedral).

Conclusions

The ligand 1,1′-bis(oxodiphenylphosphoranyl)ferrocene, odppf, appears to form two types of bischelate complexes with copper-

(22) Schwarz, W. M.; Shain, I. *J. Phys. Chem.* **1965**, *69*, 30.

(II). Moreover, the ESR data reveal that the copper(II)-oxygen bonds are scarcely covalent in character. This observation, though not surprising in copper(II) chemistry, turns out to be astonishing when considered in the frame of copper(I) chemistry. In fact, the ligand appears to stabilize the homoleptic species $[Cu(odppf)_2]^+$, which stands as the first copper(I) complex to be stabilized by a purely *hard* coordination sphere. The remarkable stability of this complex allows its synthesis along facile chemical and electrochemical routes, and reveals once more the marked borderline character of copper(I).[1] On the other hand, the complex exhibits a so marked reactivity toward dioxygen to let one to image it as a promising candidate for the constructive activation of the O_2 molecule. It is well-known that the interaction of molecular oxygen with transition metals and the formation and reactivity of dioxygen−metal compounds are important steps in a variety of synthetic, industrial and biological processes.[23] This aspect of the chemistry of **3** together with its detailed characterization will be the subject of forthcoming papers.

Acknowledgment. The authors are indebted to professor S. Aime for help in carrying out the solid-state NMR measurements. Partial support of this work by Progetto Finalizzato Chimica Fine II, Consiglio Nazionale delle Ricerche, Rome, and by Ministero Università e Ricerca Scientifica, Rome, is gratefully acknowledged.

Supporting Information Available: Tables S1−S7, listing details of the structure determinations, bond lengths, bond angles and anisotropic temperature factors (17 pages). Ordering information is given at any current masthead page.

IC950151G

(23) Kitajima, N.; Moro-Oka, Y. *Chem. Rev.* **1994**, *94*, 737 and references therein.